

Upper limits on neutron and γ -ray emission from cold fusion

M. Gai*, S. L. Rugari*, R. H. France*, B. J. Lund*, Z. Zhao*, A. J. Davenport†, H. S. Isaacs† & K. G. Lynn‡

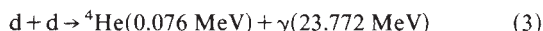
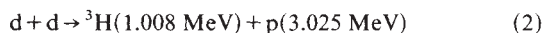
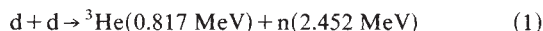
* A. W. Wright Nuclear Structure Laboratory, Yale University, New Haven, Connecticut 06511, USA

† Department of Applied Science, Brookhaven National Laboratory, Upton, New York 11973, USA

‡ Department of Physics and Applied Science, Brookhaven National Laboratory Upton, New York 11973, USA

Neutron and γ -ray emission from a variety of electrochemical cells (running continuously for up to two weeks) have been measured using a sensitive detection system with a very low background. Titanium alloy powder deuterided at room temperature and high pressure was also used for comparison. No statistically significant deviation from the background was observed in either γ -ray or neutron detectors. The estimated neutron flux in this experiment is at least a factor of 50 times smaller than that reported by Jones *et al.* and about one million times smaller than that reported by Fleischmann *et al.* The results suggest that a significant fraction of the observed neutron events are associated with cosmic rays.

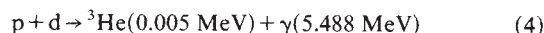
It has been suggested recently^{1,2} that deuterium in hydride-forming metals (palladium and titanium) can undergo nuclear fusion at room temperatures to release heat, neutrons, tritium and helium. Deuterium was incorporated into the metal lattices by electrolytic charging in solutions of heavy water. The nuclear reactions between deuterium nuclei that are energetically feasible (the 'open channels') are as follows:



Reactions (1) and (2) take place at similar rates³, as suggested by room-temperature muon-catalysed fusion in molecular

hydrogen¹ whereas reaction (3) can be assumed to be 4 to 5 orders of magnitude slower. Nuclear-fusion events must be characterized by the production of the ionizing radiations listed above, as there is no known mechanism that inhibits their emission.

It has been suggested that interactions between protons and deuterons,



could also take place (at a faster rate) in metals charged with deuterium (and hydrogen) from heavy water (refs 4, 5 and S. E. Koonin, personal communication). Even if the hydrogen content in heavy water is small, significant concentration of hydrogen in the metal can take place because the rate of hydrogen-ion reduction on the cathode surface is greater than that of deuterium ions by up to a factor of 13 (ref. 6), and the diffusion rate of deuterium in Pd is only a factor of 2 larger than that of hydrogen⁷.

Jones *et al.*¹ reported that, in their cells, neutrons from reaction (1) are detected at a small average rate of 2 counts h^{-1} above background. In one experiment (run 6) they report a rate of 15 counts h^{-1} for neutrons of energy $2.5 \pm 1 \text{ MeV}$. With neutron detection efficiency of 1% and using a Ti electrode of mass 3 g, they quote a cold fusion rate for $d + d$ of $\lambda_f \approx 10^{-23}$ fusions per deuteron pair per second (ref. 1). Fleischmann *et al.*² estimated a larger neutron flux of 4×10^4 neutrons per second from a 15-g Pd rod, measured with a neutron dosimeter with a detection efficiency of 2.4×10^{-6} .

Here we report on a search for neutrons and γ -rays emitted during conjectured fusion of $d + d$ and $p + d$ in various metals into which deuterium has been incorporated ('deuterided' metals). Measurements were carried out with an array of low-background, high-sensitivity neutron detectors and two large high-efficiency NaI(Tl) γ -ray detectors. The contribution from

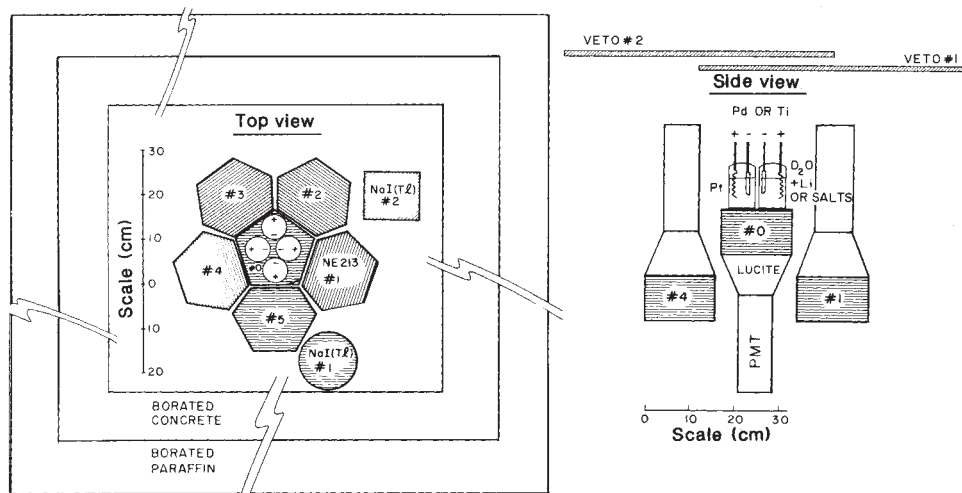


FIG. 1 Schematic diagram of the experimental setup, drawn to scale.

cosmic rays was measured with two large-area cosmic-ray veto counters. Four cells were used concurrently, with electrodes and solutions based on those used in the experiments reported by Jones *et al.*¹ and Fleischmann *et al.*². In addition, one Ti alloy powder sample deuterided by gas-phase deuterium was used (see Table 1 footnote). We report here on data taken over a period of three weeks. We observe no statistically significant excess of counts of either neutrons or γ -rays above the background, and we have obtained upper limits on the rates of cold fusion in deuterided palladium and titanium.

The detector system

The neutron detector system is shown in Fig. 1. It consists of six NE213 liquid-scintillator neutron counters with fast-photo-multiplier tubes selected from the Yale neutron ball⁸. Each detector was 10 cm thick. The central detector (number 0) was a regular pentagon (inscribed in a circle of radius 9 cm). The four electrolytic cells were placed on this detector with the palladium or titanium cathodes close to the centre, for maximum efficiency of neutron counting. The other five detectors (numbers 1 to 5) were irregular hexagons with dimensions similar to that of detector 0. These were arranged in a ring displaced 15 cm below detector 0.

State-of-the-art pulse-shape-discriminator electronic modules (ref. 9; modules produced by W. F. Piel) were used to distinguish between neutrons and γ -rays. A hardware gate was used to discard almost all detected γ -ray events in each detector. The efficiency of the neutron detectors was measured with calibrated neutron sources: ^{252}Cf (neutron energy $E_n = 2 \pm 1$ MeV) and Pu-Be ($E_n = 4 \pm 2$ MeV)¹⁰ placed in the middle of the four cells above the centre of detector 0. The efficiency is sensitive to the value of the threshold, which was set at ~ 80 – 100 keV (electron equivalent), corresponding to neutron energies of 400–500 keV (ref. 11). The average efficiency of the detectors was measured as $\sim 25\%$ for neutrons from the ^{252}Cf source, in agreement with the value calculated from a simple model¹¹. The efficiency of individual detectors ranged between 16% and 36%, reflecting individual thresholds and detector performance. The possibility that the detectors were only sensitive to the higher-energy neutron tail of the ^{252}Cf source can be excluded, as the spectrum includes less than 7% of neutrons with energies in excess of 2.5 MeV (ref. 10).

The detection of neutrons is characterized as a coincidence event between a primary neutron registered in detector 0 and a scattered neutron (with approximately half the energy of the primary neutron, as a result of detector geometry) detected in one of the detectors 1 to 5. A neutron event is then defined by measuring its pulse shape in the second detector, the pulse heights in the two detectors, and the time of flight between the two detectors, which is related to the energy of the neutron. The coincidence method significantly lowers the background in the detector system and at the same time yields a reasonable efficiency (discussed below). The time differences (t) between successive events in detector 0 and any one of the detectors 1 to 5, for neutrons from a Pu-Be neutron source, are shown in Fig. 2a, and from a ^{252}Cf neutron source in Fig. 2b. The raw data include γ -ray (γ - γ') and neutron scattering events (n - n'). Gamma-ray-neutron coincidences (γ - n) are also evident in the spectrum. The γ - γ' time resolution was measured, using standard γ -ray sources (^{60}Co , ^{133}Ba and ^{137}Cs), to be ~ 2.5 ns; an appreciable contribution to the observed time resolution comes from 'electronics walk' as a result of the low threshold. In Fig. 2c we show the time spectrum gated by the neutron pulse shape of detectors 1–5. We are clearly able to remove γ - γ' coincidence events in the source data (these appear in Fig. 2b) by using this software gate on the pulse shape, without significantly affecting the n - n' coincidence events. The time of flight between detectors whose centres are 20 cm apart can be estimated on the assumption that the scattered neutron emerges with 50% of the energy of the primary neutron. The value expected for a 1-MeV neutron (^{252}Cf source) is $\Delta t = 14$ ns and for a 2-MeV neutron (Pu-Be source) is $\Delta t = 10$ ns. These are in approximate agreement with the centroid separation of the n - n' and γ - γ' peaks shown in Fig. 2.

The total efficiency of the neutron detection system in n - n' coincidence mode was measured using a ^{252}Cf source to be $1.0 \pm 0.2\%$ which is similar to that of Jones *et al.*¹. Neutron-neutron coincidences from two primary neutrons from the ^{252}Cf source (emitting 3–4 neutrons per fission) are suppressed by a factor of 16 because of the small solid angle over which measurements are made, and thus do not affect our measured efficiency. This value of the efficiency is consistent with a solid angle of 30% of 4π for detector 0, a solid angle of 45% of 2π for the ring of detectors 1–5 and an average intrinsic efficiency of 25%

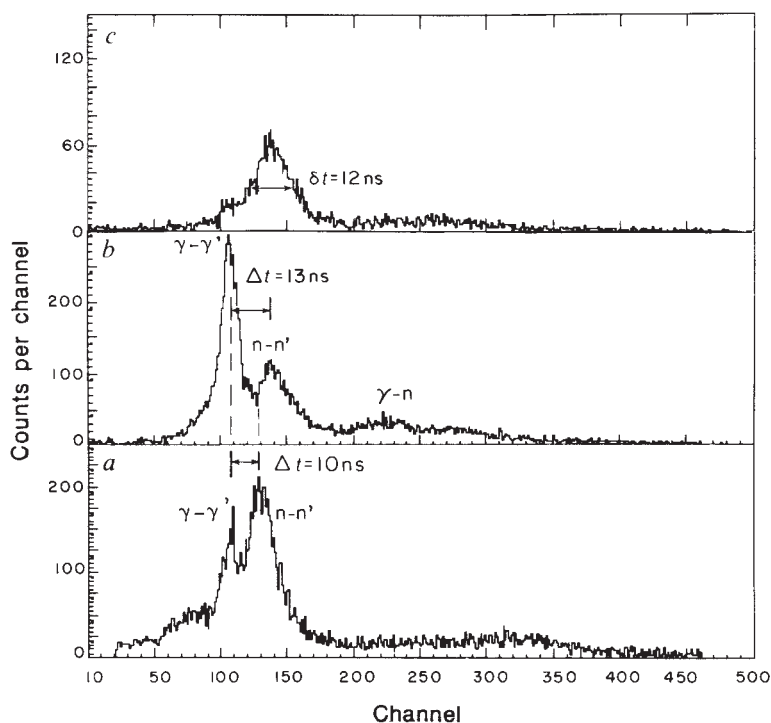


FIG. 2 Typical time-of-flight spectra measured with a, Pu-Be, and b, ^{252}Cf neutron sources, and c, with a cut on the neutron pulse shape, for the ^{252}Cf data. The time calibration is 2.5 channels per ns, with $t=0$ defined at the location of the n - n' peak. In a and b, Δt is the neutron time of flight. In c, δt is the width of the neutron time-of-flight distribution.

for the individual detectors. Calibration spectra were measured every 1–2 days to ensure that no drifts occurred in the system.

The neutron counting rate in each detector was ~ 120 counts h^{-1} over the entire energy range of the detector (for neutrons of energy < 6 MeV). In the coincidence-time spectra the rates are less than 1 count h^{-1} in each pair of detectors and, on average, 1.6 counts h^{-1} in the entire array of all five pairs. All five time spectra between detectors 0 and 1–5 were summed at the end of each run. The neutron events are summed in a region extending from the γ - γ' peak (defining time of flight $t \approx 0$ ns) to $t = 40$ ns (that is, 100 channels beyond this peak). The latter boundary corresponds to the largest flight time possible for neutrons of lowest energy (400–500 keV, that is, just above the detection threshold).

Two large-volume 12.5 \times 12.5 cm NaI(Tl) detectors, with a resolution of 7% at 1.33 MeV and total full-energy peak efficiency (for each detector) of 0.1% at 5.5 MeV, viewed the cells directly at a distance of 32 cm, as shown in Fig. 1. Two large-area, 6-mm-thick, plastic-scintillator veto-counters, with dimensions of 120 \times 60 cm and placed 35 cm above detector 0, were used to detect energetic cosmic rays traversing the apparatus, with a veto gate extending for 3 μs . These detectors subtended an angle of $\pm 60^\circ$ above the samples, with a veto efficiency of about 65%. The veto efficiency was measured using the high-energy portion (31-MeV) of the NaI(Tl) spectra, as shown in Fig. 3. In this region the count-rate is due to cosmic-ray interactions and the veto efficiency is given by the ratio of the two rates (Fig. 3).

Data were collected event-by-event on a Concurrent 3230 computer and stored on tape for later analysis. Each recorded event includes up to 20 parameters. Pulse-shape and pulse-height data were recorded using two 8-channel ORTEC AD811 analog-to-digital converters, and time-of-flight data were recorded using an 8-channel LECROY 2228A time-to-digital converter. The data collected during runs 8–14 were accumulated using a CAMAC crate interfaced to an IBM PC/AT compatible (20 MHz) Dell 310 computer with histogramming capability only.

Data were taken in two-hour run periods which were recorded and examined individually before being summed. Background was measured under various conditions: with cells removed from the shielded area containing the detectors (run 2), with cells in their normal position but passing no current (run 5), and with a cell including heavy water and LiI salt without electrodes (run 4). This last cell was used to assess the effects of cosmic rays on cells that included material with a large atomic weight.

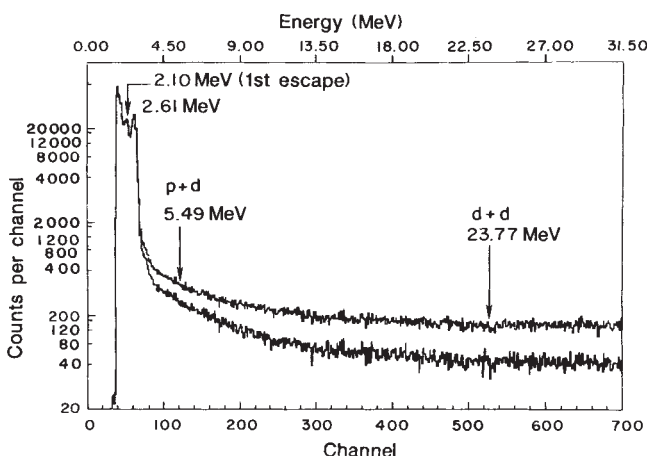


FIG. 3 Typical spectra from NaI(Tl) γ -ray detector 2 (run 6). The locations of the expected γ -rays from reactions listed in text are indicated. The raw γ -ray counts before and after vetoing on cosmic rays correspond to the upper and lower curves respectively.

The detector system was enclosed in a shielded housing of 15-cm-thick borated concrete and 15-cm-thick borated paraffin, and was covered with two layers of 15-cm-thick borated paraffin blocks. No lead shielding was used as this was found to increase the background. The housing's outer dimensions were 150 \times 150 \times 150 cm. The experiment was carried out in a target area of the A. W. Wright Nuclear Structure Laboratory (with the tandem accelerator not running) under a 90-cm-thick roof composed of steel-reinforced concrete.

In the following we outline the procedures used in applying cuts on the data. Run 7 contains data from cell number 1 (running for 15 days), cells 2–4 (running for 1–4 days), and sample 9 (see Table 1) on the detector. In Fig. 4a we show the raw data as registered in the first channel of the time-to-digital

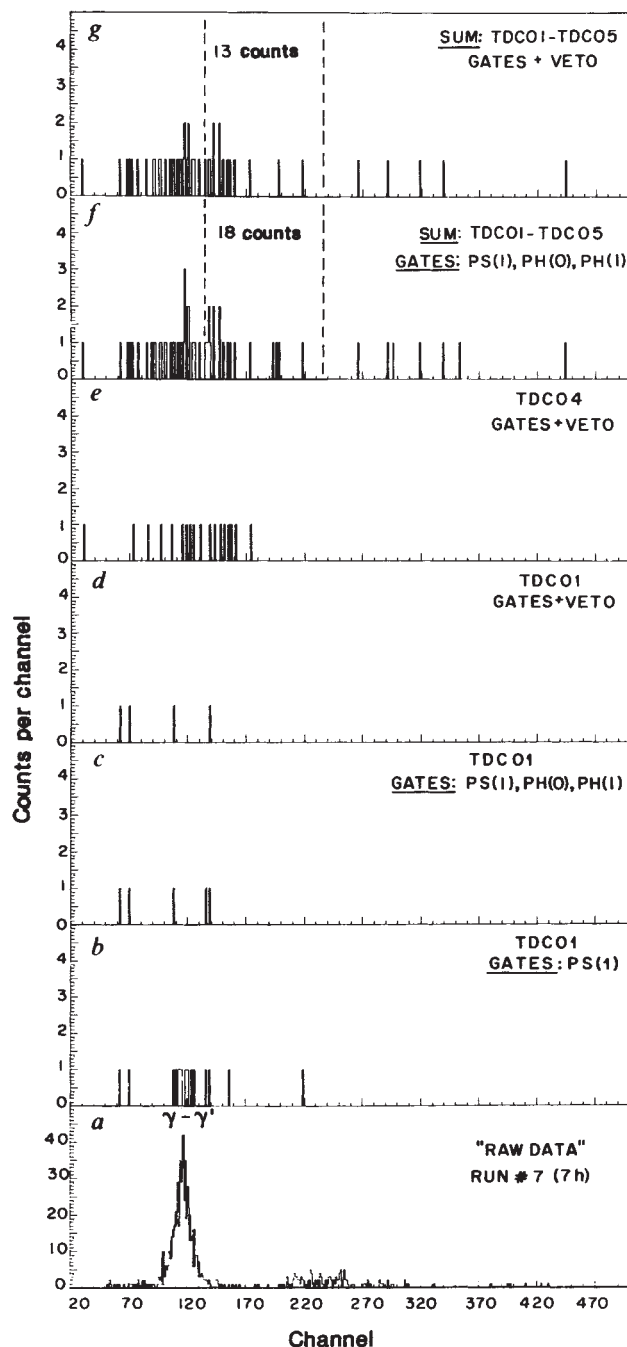


FIG. 4 Time spectra obtained during run 7 with cells on, with various gates and veto conditions as indicated, and discussed in text. The time range of interest, which brackets maximum and minimum times of flight of neutrons of about 2.5 MeV (discussed in text) is indicated by the vertical dashed lines.

TABLE 1 Measurements and elapsed times for charging electrodes (5–26 May 1989)

Run	Electrodes	Electrolytes	Charging time (h)	Counting time (h)	Run	Electrodes	Electrolytes	Charging time (h)	Counting time (h)
0*	1	3	up to 192	up to 60	8#	1	3	346	10.0
	2	5	up to 72	up to 60		3	1	155	10.0
	5	3	up to 72	up to 60		7	3	155	10.0
	6	5	up to 72	up to 60		4	2	77	10.0
1	1	3	192	20.3	9	1	3	356	7.2
	3	1		20.3		3	1	165	7.2
	7	3		20.3		7	3	165	7.2
	2	4	24	20.3		4	2	87	7.2
2†	1	3	216	9.7	10	1	3	364	17.3
	3	1	24	9.7		3	1	173	17.3
	7	3	24	9.7		7	3	173	17.3
	2	4	47	9.7		4	2	95	17.3
3‡	1	3	226	15.3	11	1	3	382	8.5
	3	1	34	15.3		3	1	191	8.5
	7	3	34	15.3		7	3	191	8.5
	8	5		15.3		4	2	113	8.5
	9					12	1	3	391
4§	None	10	6.1	3	1		200	11.9	
5	4	2		11.9	7	3	200	11.9	
6	1	3	270		4	9	122	11.9	
	3	1	78		13**	1	3	411	23.5
	7	3	78			3	1	220	23.5
	4	2		28.6		7	3	220	23.5
7¶	1	3	299	7.0		4	9	142	23.5
7¶	3	1	107	7.0	14	1	3	435	21.4
	7	3	107	7.0		3	1	244	21.4
	4	2	29	7.0		7	3	244	21.4
	9					4	9	166	21.4

ELECTRODES. (1) Pd plate 1×5×50 mm, cold-worked and heated in D₂ at 120 p.s.i. and 300 °C, and furnace-cooled under pressure (D/Pd=0.73), immersed to 3.1 cm, (active area=3.7 cm²), anodized at 1 mA for 10 min. Electrical connections made with spot-welded Type 308 stainless steel rod, 3 mm in diameter. (2) Pd cylinder, 2 mm diameter, 100 mm long, annealed in flowing argon at 1,000 °C, immersed to 3.1 cm (active area=1.9 cm²), anodized at 1 mA for 10 min. (3) Pd cylinder, 6 mm diameter, 50 mm long, annealed in flowing argon at 1,000 °C, exposed to 120 p.s.i. D₂, anodized at 1 mA for 10 min., immersed to 3 cm (active area=5.8 cm²). Electrical connections as in (1). (4) Pd cylinder, 6 mm diameter, 50 mm long, with reduced section 2 mm diameter for electrical connection, annealed in vacuum at 900 °C, anodized at 50 mA for 10 min, immersed to 3 cm (active area=5.8 cm²). (5)–(8) Ti parallelepiped 3×3×45 mm, cold-worked, immersed 3 cm (active area=2.8 cm²). Electrical connections as in (1). (9) TiFe_{0.7}Mn_{0.2} powder (43 g) hydrided at 120 p.s.i. D₂, at room temperature, charged on 19 December 1987 and recharged on 4 April 1989. Contained in a 2 cm×20 cm cylinder. Etch for Ti: 5% HF (48%) in H₂O₂ (10 vol). Etch for Pd: 40% HNO₃ (98%): 60% HCl (36.5%).

ELECTROLYTES. (1) 0.1M LiOD/97.5% D₂O. (2) 0.1M LiOD/99.8% D₂O. (3) 1M LiOD/97.5% D₂O. (4) 1M ⁹LiOD/97.5% D₂O. (5)–(8) 100 g 97.5% D₂O + 0.125 g FeSO₄·7H₂O, 0.125 g NiCl₂·6H₂O, 0.125 g PdCl₂, 0.125 g Li₂SO₄·H₂O, 0.125 g Ti(SO₄)₂·9H₂O, 0.35 g CaSO₄, 0.11 g NaH₂PO₄, 0.125 g CaCO₃ adjusted to pH<3 with HNO₃. (9) 0.1M LiOD/99.3% D₂O. (10) Lil solution (30 g) in 100 cm³ heavy water. No electrode used.

* While experimental setup was improved, cells were on and counting was carried out with a reduced detector system. In this period five experiments were performed with the above electrode etched and abraded.

† Cells were moved out of shielded counting system, but cells remained on in a second, well shielded housing. Calibration measured.

‡ Cells were moved back into shielding together with sample 9, electrode 2 was replaced with 8. Calibration measured, cells on continuously.

§ Cells were run with electrodes 1, 3 and 7 outside of counting area. Calibration and background measured. Cells on continuously.

|| Cell off.

¶ Three cells returned to counting area, together with sample 9. Calibration measured, cells on continuously.

Counting system reduced to include only TAC01, PSDO and NaI₂. Read by an IBM PC/AT compatible.

** Sample of heavy water (5 cm³) was taken for analysis from cells 1 and 4.

converter (TDC01), corresponding to the time of flight between two detectors, measured between a (common) start signal from detector 0 and a stop signal from detector 1. In these data we again observe the γ - γ' peak (defining time $t \approx 0$). Neutrons are expected in up to 100 channels beyond this peak, as discussed above. The background signal around channel 250 is due to the low threshold used in this experiment and arises from γ - γ' events. By using a software gate on the neutron pulse shape of detector 1 such that only neutrons are detected in this detector, we get the data shown in Fig. 4b, and by excluding neutrons of energies larger than 3 MeV, we get the spectra shown in Fig. 4c. This yields a neutron detection rate in the 0–1 pair of 3 counts in 7 h (note that these counts cannot all be resolved by eye in Fig. 4). The cut on higher-energy neutrons removes n–n' scattering events in the vicinity of the γ - γ' peak ($t \approx 0$), because higher-energy neutrons are fast. By vetoing of cosmic-ray events we are left with 2 neutron events in the region of interest (corresponding to the largest and smallest possible flight times,

and shown by dashed lines in Fig. 4f, g) after 7 h of counting in the 0–1 neutron detector pair (Fig. 4d). The 0–4 neutron-detector pair generally showed a higher counting rate (because of its larger measured efficiency), yielding 6 neutron events in 7 h (Fig. 4e). In the whole array, we obtained 13 counts for 2.5-MeV primary neutrons (Fig. 4g) in the area of interest, giving a neutron rate of 1.8 ± 0.4 counts h⁻¹.

Electrochemical procedures

The electrochemical cells used in this experiment were contained in 100-ml polyethylene bottles. The top of each bottle held the cathode (palladium or titanium, more than 99.9% pure), the anode (several strands of 0.5-mm-diameter platinum wire in an S-shape), a fine tube for the introduction of nitrogen gas presaturated with heavy water, and a vent hole for the nitrogen mixed with the gaseous electrolysis products. The flow rate of nitrogen through the cell was sufficient to dilute the deuterium gas to a concentration below 5%, thus reducing the risk of explosion.

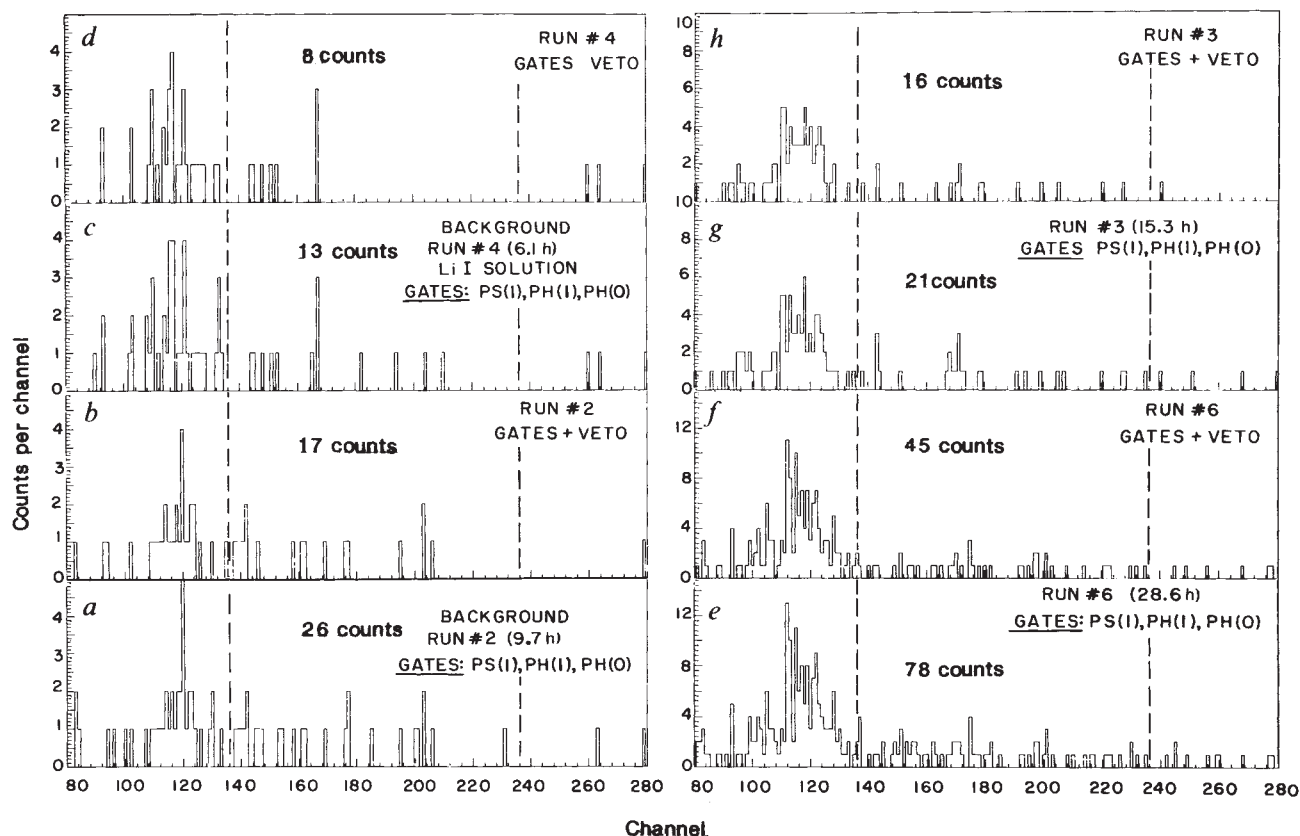


FIG. 5 Time-of-flight spectra obtained for various runs, both with cells on and off (background runs). The data in *g* were obtained under conditions

similar to those in ref. 1. For further details, see text.

The connections, dimensions and pre-treatments of the palladium and titanium cathodes are listed in Table 1, and included etching and electrode treatments. Two types of electrolyte were used: LiOD (ref. 2) and a complex mixture of salts with an acidic pH, based on that used in ref. 1. LiOD solutions were made by adding lithium metal to D_2O . The compositions of the different solutions used, and the 'cell-on' and counting times, are listed in Table 1.

A constant current was provided by PAR 363 potentiostat-galvanostats. A current of 300 mA was used for all the cells except that including electrode 4, for which 500 mA was used. The cell voltages varied between 3 and 15 V, the higher values being found for electrolytes of low ionic strength. Heavy water was periodically added to the cells (a few cm^3 per day) to replace the heavy water lost through electrolysis. The H:D ratio in LiOD solutions was found by NMR techniques to be $\sim 2.5\%$ after one week of running time. One sample (9) of deuterided Ti alloy powder was used for comparison with the electrochemically charged cells. This powder sample was deuterided at room temperature rather than at low temperature, in contrast to the experiments of De Ninno *et al.*¹²

Results

Figure 5a shows background data measured over 9.7 h (run 2) with no cells in the shielded housing. This figure shows only the final gated and vetoed data, as discussed above. Data taken with only the solution of LiI salt (run 4) are shown in Fig. 5c. Background data with an uncharged cell in place and with electrode 4 in solution 2 (run 5) (not shown in Fig. 5) yield no statistically significant difference in the neutron rate. In Fig. 5e we show the results obtained by using one cell containing solution 2 with higher-purity heavy water (99.8%) in conjunction with the pre-treated electrode 4 (run 6). In Fig. 5g we show the data (run 3) obtained from cells and solutions similar to those used by Jones *et al.*¹ (see Tables 1 and 2). In Fig. 6 we show neutron count rates with background subtracted for all runs 1–14, spanning almost three weeks of data collection. Cells were charged for a few days before run 1 (see Table 1), and the neutron rates at that time were typically 1 ± 1.5 counts h^{-1} above background (not shown in Fig. 6). In several runs, we used solutions and electrodes with surface and chemical treatments similar to those used by Jones *et al.* Although in some respects

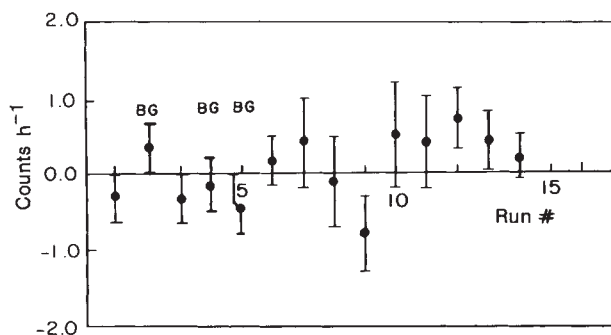


FIG. 6 Neutron count rates above average background rate (1.4 counts h^{-1}). The average rate is 0.1 ± 0.2 counts h^{-1} above background, which is significantly smaller than Jones *et al.*¹, who had the same measuring efficiency of 1%. BG indicates background runs.

our experimental arrangement may differ slightly from that of Jones *et al.* (for example, we used a platinum rather than gold electrode), the relevant features are similar. No statistically significant effect above background was observed. The average neutron count rate above background for run 6 is 0.1 ± 0.2 counts h^{-1} , a factor of 50–100 below the 15 counts h^{-1} reported by Jones *et al.*, who had a similar efficiency of 1%.

The vetoed neutron rates (at 2.5 MeV) are $\sim 35\%$ of the total detected neutron rate (Fig. 5). With the measured veto efficiency of 65% (Fig. 3), it is possible that the major portion of our neutron events (at least 50%) are induced by cosmic rays. However, as can be seen in Fig. 5, the same vetoed-event rates were observed with and without cells in the detection system, and hence it is not possible to attribute these events solely to the interaction of cosmic rays in the electrodes. We note only that cosmic rays yield neutrons of energies 1–3 MeV at a rate of ~ 1 –2 counts h^{-1} . Our sensitivity would suggest that less than 10% of these neutrons are produced by interactions of cosmic rays in the cell alone. This rate (1–2 counts h^{-1}) is only slightly below the average rate (above background) of 2 counts h^{-1} reported by Jones *et al.*, measured at a higher altitude in Utah. In addition, the presence of a peak in the spectrum of cosmic neutrons with energies of a few MeV is well-known¹³. Although time variations of cosmic-ray distributions are small, it is still possible that variations in the effect of cosmic rays in the experimental arrangement of Jones *et al.*, or barometric changes¹⁴, could account for the small effect that they reported.

These data can be used to set upper limits on d+d fusion. In particular, the data of run 6 (Fig. 5f) yielded 1.6 ± 0.2 counts h^{-1} . The average background rate (runs 2, 4 and 5) was 1.4 ± 0.2 counts h^{-1} . This yields an upper limit on the count rate resulting from the cells of 0.2 ± 0.3 counts h^{-1} above background, or a 3σ limit of 1.1 counts h^{-1} . The cell in run 6 (cell 4) includes electrode 4, consisting of 10.2 g Pd. With the assumption that the d: Pd ratio in the deuterided electrode is unity¹⁵, our neutron efficiency (1%) yields an upper limit for the cold fusion of d+d in deuterided Pd metals (at 98% confidence) of $\lambda_f < 1 \times 10^{-24}$ fusions per atom pair per second. Run 3 includes a cell similar to that used by Jones *et al.*, with two Ti electrodes of mass 2.4 g (7 and 8; see Table 1). We obtain a rate of 1.0 ± 0.2 counts h^{-1} (-0.4 ± 0.4 counts h^{-1} above background) for this run. With the assumption that the titanium has been converted to the γ -TiD₂ structure with the ratio d: Ti = 2, this yields an upper limit on the d+d fusion in charged Ti (at 98% confidence) of $\lambda_f < 6 \times 10^{-25}$ fusions per atom pair per second. Summing runs 1, 3, 6 and 7 (spanning 71.2 h of counting), with a neutron rate of 1.3 ± 0.1 counts h^{-1} (-0.1 ± 0.2 counts h^{-1} above background), we arrive at an upper limit for d+d cold fusion in deuterided Pd and Ti (at 98% confidence) of

$$\lambda_f < 2 \times 10^{-25} \text{ fusions per atom pair per second} \quad (5)$$

This rate is nearly two orders of magnitude below that suggested by Jones *et al.* ($\lambda_f \approx 10^{-23}$ fusions per deuteron pair per second). Similar limits were obtained in gases¹⁶ for molecular HD

($< 10^{-24}$ fusions per molecule per second) and for molecule D₂ ($< 10^{-26}$ fusions per molecule per second).

The γ -ray data shown in Fig. 3, from run 6 extending over 28.6 h, with the total full-energy peak efficiency at 23.8 MeV of 0.02%, yield an upper limit on the emission of γ -rays from the fusion of d+d of $\lambda_f < 2 \times 10^{-20}$ fusions per atom pair per second; here we assume that reaction channel (3) has a branching ratio of 10^{-4} . The background at the range of interest (23.8 MeV) is ~ 1 count h^{-1} per channel and the energy resolution (full width at half maximum) at this region corresponds to 6 channels. The γ -ray rate at 5.5 MeV was measured in run 13 (at which time the residual activity in the detector from ²⁴Na, produced by successive neutron calibration, was small). With the cells that contain 2.5% normal water and with the separation factor of 13 (ref. 6) this leads to a ratio D: H = 3; here we have assumed that deuterium and hydrogen are distributed uniformly throughout the lattice. With the above assumptions and using the upper limit on the γ -ray count-rate above background (see Fig. 3), we arrive at the upper limit for the fusion of p+d (at 98% confidence) of

$$\lambda_f < 1 \times 10^{-22} \text{ fusions per atom pair per second} \quad (6)$$

For a smaller separation factor of 4, the upper limit will be increased by a factor of 3.2. The p+d reaction rate of molecular hydrogen isotopes was calculated to be 10^8 times faster than the d+d reaction rate (refs 4, 5); in metals it is only 10^2 times faster (ref. 4 and S. E. Koonin, personal communication). Together with the d+d fusion rate suggested by Jones *et al.*¹, we would expect the p+d rate to be $\sim 10^{-21}$ fusions per atom pair per second, a factor of 10 greater than our measured upper limit.

Conclusions

We have carried out a number of tests of some of the claims regarding cold fusion made by Fleischmann *et al.*² and Jones *et al.*¹. We have attempted to reproduce the electrochemical conditions used by them, and have also used a sample deuterided under high-pressure gas. We have searched for the neutrons and γ -rays that must be emitted from the putative cold-fusion processes. Our experiments, with high sensitivity and small background, have revealed no statistically significant deviation from background. The upper limits that we deduce for the rates of cold fusion of d+d and p+d in metals are considerably smaller than those reported in refs 1 and 2. The average neutron detection rates above background reported by Jones *et al.*¹ (measured with the same efficiency as here) are consistent with the rate that we measure for neutrons originating from cosmic rays. It is therefore likely that a significant fraction of the neutrons measured by Jones *et al.* may be attributed to cosmic rays. The absence of neutrons and γ -rays emitted from these cold-fusion systems, together with the absence of a known mechanism for the suppression of reactions (1), (3) and (4), raises serious doubts as to whether cold fusion does occur in deuterided Pd and Ti metals at the rates suggested by Fleischmann *et al.*² and Jones *et al.*¹. \square

Received 17 May; accepted 12 June 1989.

- Jones S. E. *et al.* *Nature* **338**, 737–741 (1989).
- Fleischmann, M., Pons, S. & Hawkins, M. *J. electroanal. Chem.* **261**, 301–308 (1989); and erratum.
- Fiarman, S. & Meyerhof, W. E. *Nucl. Phys. A* **206**, 1–64 (1973).
- Koonin, S. E. & Nauenberg, M. *Nature* **339**, 690–691 (1989).
- Picker, H. S. *Nukleonika* **25**, 1491–1493 (1980).
- Dandapani, B. & Fleischmann, M. *J. electroanal. Chem.* **39**, 323 (1972).
- Wicke, E. & Brodowsky, H., in *Hydrogen in Metals II* (eds Alefeld, G. & Völkl, J.) 73 (Springer, Berlin, 1978).
- Rugari, S. L. thesis, Yale Univ.
- Pai, S., Piel, W. F. Jr, Fossan, D. B. & Maier, M. *Nucl. Instrum. Meth.* (in the press).
- Hanson, A. O. in *Fast Neutron Physics* (eds Marion J. B. & Fowler, J. L.) 3 (Interscience, New York, 1960).

- Finckh, E. in *Nuclear Spectroscopy and Reactions* (ed. Cerry, J.) 573 (Academic Press, New York, 1974).
- De Ninno, A. *et al.* *Europhys. Lett.* (submitted).
- Hess, W. N., Patterson, H. W. & Wallace, R. *Phys. Rev.* **116**, 445–457 (1959).
- Carpenter, J. M. *Nature* **338**, 711 (1989).
- Hoare, J. P. & Schuldiner, S. *J. electrochem. Soc.* **102**, 485 (1955).
- Champagne, A. E., Howard, A. J. & Parker, P. D. *Bull. Am. phys. Soc.* **26**, 564 (1981).

ACKNOWLEDGEMENTS. We acknowledge useful discussions with P. D. Bond, D. A. Bromley, S. Feldberg and P. D. Parker. We wish to thank J. S. Greenberg for helpful discussions, R. D. Mařka and R. K. Adair for providing the veto counters, B. W. Bangertner for making the NMR measurement of the H:D ratio in the solution and supplying research-quality heavy water, and J. Reilly for preparing sample 9. The work was supported in part by the US Department of Energy.